ELSEVIER

Polymer 43 (2002) 4103–4110

polymer

www.elsevier.com/locate/polymer

Modelling the structural and physicomechanical properties of substituted poly(*p*-phenylene)s using molecular mechanical and molecular orbital methods

S. Hill, I. Hamerton, J.N. Hay, B.J. Howlin*

Department of Chemistry, School of Physics and Chemistry, University of Surrey, Guildford GU2 7XH, UK

Received 24 October 2001; received in revised form 24 January 2002; accepted 5 April 2002

Abstract

Conducting polymers are important technological materials that are finding increasing use in batteries and display devices. The conformation and packing of these polymers in the amorphous glassy state are poorly understood, despite the fact that they dictate their most important physical and mechanical properties. The processing of currently known conducting polymers is difficult and there is a strong incentive to increase their processability through functionalization. Developing an ability to predict the structure and structure–property relations of conducting polymers in the bulk will help with the design of new structures that combine processability with favourable electronic properties and facilitate their use in future high-technology applications. In this work, we concentrate on substituted poly(*p*-phenylene)s. Detailed atomistic molecular models have been developed with the help of molecular mechanics and semi-empirical quantum mechanical calculations using Cerius and MOPAC V6.0 program packages and structural, volumetric, and mechanical properties, e.g. geometrical values, densities, have been calculated by simulations on these models. The results from both methods have been compared with simulated and experimental data and conclusions have been drawn on the methodology and the approximations used. This study was used to compare with results obtained on unsubstituted poly(*p*-phenylene)s carried out earlier and to continue to develop our methodology for calculating structure, physical and mechanical properties that will be generally applicable to conductive polymers. © 2002 Published by Elsevier Science Ltd.

Keywords: Modelling; Quantum and classical mechanics simulation; Conductivity

1. Introduction

One of the major developments in physical sciences during the last 15 years has concerned the growing ability of computational techniques to model the behaviour of matter at the atomic level. Polymers with conjugated backbones display unusual electronic properties such as low energy optical transitions, low ionization potentials, and high electron affinities. The result is a class of polymers, which can be oxidized or reduced more easily and more reversibly than conventional polymers. A significant breakthrough occurred in 1979 with the discovery [1] that poly(*p*-phenylene) could also be doped to achieve high conductivity. Poly(acetylene) [2] demonstrated that it was not unique and this led to a number of new polyaromatic based conducting systems, including poly(pyrrole) [2,3], poly(thiophene) [4], and poly(aniline) [5]. Electronically conducting polymers are an extremely promising category of materials for, by controllably adjusting their doping level, one can achieve conductivities anywhere between insulating and metallic values. At the same time, they offer the potential of being easily and inexpensively processed, e.g. through extrusion, fibre spinning or spin coating, as ordinary thermoplastic polymer coatings. In practice, however, most electronically conductive polymers are not readily processed in their pure form. To achieve processability, they are usually blended with more common, non-conducting polymers. Chemical functionalization, e.g. the introduction of side chains that induce liquid crystalline behaviour, is another strategy for improving processability. In this work, we concentrate on the chemical functionalization approach. A method called the Durham route involves the reaction with pendant groups that do not break the main polymeric backbone [6–9]. However, blending and functionalization generally affect the electrical conductivity. Thus a major technological issue is how to design polymeric systems that display the best combination of electronic and processability properties for specific applications. Although high-capacity poly(pyrrole) capacitors and

* Corresponding author. Tel.: 1483-876-834; fax: 1483-876-851.
E-mail address: b.howlin@surrey.ac.uk (B.J. Howlin).

0032-3861/02/$ - see front matter © 2002 Published by Elsevier Science Ltd.
PII: S0032-3861(02)00244-6

rechargeable poly(aniline) batteries are in commercial production, it is generally thought that the potential of conducting polymers has not nearly been tapped, e.g. poly(*p*-phenylene sulphide) possesses unusual chemical resistance properties, compared with previously used poorer materials such as metals. Another particular advantage of this type of conducting polymer is its resistance to prolonged exposure to direct sunlight. Conducting polymers being applied in today's technology would include, avionics, radar systems and signal processors.[1] Innovative 'molecular engineering design' strategies are required and molecular computer modelling is a very promising avenue towards molecular engineering design, as evidenced by its rapidly increasing use in industrial settings, e.g. the pharmaceutical industry in the understanding of the complex structures of proteins. There has been a wealth of previous work on the theoretical investigation of conducting polymers. Starting from simpler systems, e.g. the modelling of biphenyls and triphenyls (as simpler models) evokes interest both from an academic and technological viewpoint, Bredas [10] has produced an overview of the study of conjugated polymers and oligomers from a quantum chemical angle. A major area of research has also focused on the electronic structures of conjugated polymers in order to understand the band gaps in these materials. To this end, the theoretical calculation of electronic structures of conducting polymers has been studied by Salanaek and Bredas [11], overviewed by Bredas [12] and applied to statistical and block copolymers of poly(*p*-phenylene) and poly(acetylene) by Quattrocchi et al. [13]. Much study on the electronic and optical properties of poly(*p*-phenylene-vinylene) polymers [14] and oligomers [15] has also been undertaken, due to the interesting non-linear optical properties of these oligomers [16]. A non-linear optical response occurs, after a charge injection, and is then followed by a structural relaxation forming these self-localized non-linear excitations. The effect of torsion angle on the structural and electronic properties of a cyano-substituted poly(*p*-phenylene vinylene) polymer has also been calculated by Fahlman and Bredas [17], although the linking group is a vinylene moiety, in this case the presence of the cyano group further complicates the issue. There is some discussion in the literature regarding the molecular orbital method best suited to calculating electronic structures, e.g. Cornil et al. [16] used the Austin Model 1 (AM1) geometries coupled with intermediate neglect of differential overlap/configuration interaction (INDO/CI) which reproduces the localization of charge carriers better than the corresponding unrestricted Hartree–Fock (UHF) method. They noted that the INDO/CI approach allowed the analysis of the linear and non-linear optical response, as this was the most interesting property according to them. In essence, the larger the basis set the better the energies, although the geometries will not necessarily improve. In the past, it has been proved that it is possible to scale semi-empirical energies to those calculated with higher basis sets, i.e. the actual energy may differ but the trend is the same. The introduction of side chains on to the aromatic rings improves their processability and also their solubility in some solvents. However, chemical functionalization can also have a deleterious effect on the conductivity of the resulting polymer. We have attempted to study this effect by selecting a range of differently functionalized poly(*p*-phenylene)s and calculating their geometric and electronic properties.

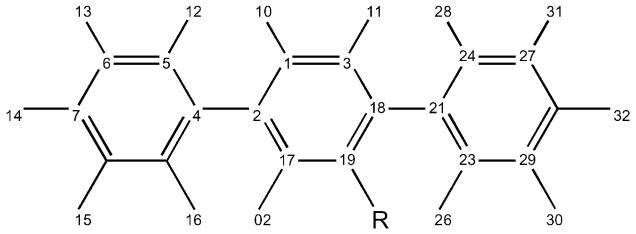

Fig. 1. Numbering of molecule.

2. Experimental

2.1. Modelling the substituted phenylene monomer

Gas phase and solid-state: The modelling work presented here was carried out on a Silicon Graphics Indigo RS4600. The software used was Cerius 2 version 2.0 and version 4.0, supplied by Molecular Simulations Inc. [18]. Models of the polymers in question were built atom by atom within the 3D Builder module of Cerius 2. Atomic partial charges were calculated using the QEq_neutral charge equilibration method [19]. The molecules were minimized using the DREIDING 2.21 force field [20], with an RMS force of 0.004 kJ mol^{-1} (1 kcal = 4.184 J). The RMS force of 0.00001 kJ mol^{-1} was also used for the –C=OBr substituted poly(*p*-phenylene) molecule. Initially, one repeat unit of each polymer was constructed and large models generated using the CRYSTAL BUILDER module in Cerius 2. Experimental data for triphenyl from X-ray crystallography were taken from the Cambridge Crystallographic Database [21] and also from studies reported by Vaschetto et al. [22–25]. The structures minimized with partial

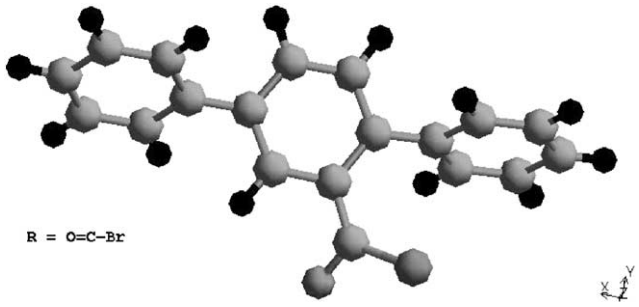

Fig. 2. Computer simulated model.

[1] www.ctscorp.com.r.interconnect.supermil.htm.

Table 1

No.	Atom	Bond/*X*	Angle/*Y*	Torsion/*Z*	Connectivity		
(a) Geometry of the tri-poly(*p*-phenylene) from chemical structural database [21]							
1	C1						
2	C22	1.502			C1		
3	C23	1.409	120.53		C22	C1	
4	C25	1.403	121.3	179.5	C23	C22	C1
5	C29	1.397	121.37	−0.7	C25	C23	C22
6	C32	1.486	121.97	−179.4	C29	C25	C23
7	C33	1.401	121.24	−179.7	C32	C29	C25
8	C35	1.407	121.6	179.6	C33	C32	C29
9	C39	1.4	120	2.4	C35	C33	C32
10	C37	1.397	118.91	−3	C39	C35	C33
11	C34	1.409	120.86	−179.5	C32	C29	C33
12	H38	1.101	126.06	170.8	C34	C32	C37
13	H41	1.089	116.64	179.4	C37	C39	C34
14	H42	1.099	121.52	−172.4	C39	C35	C37
15	H40	1.068	123.66	−175.3	C35	C33	C39
16	H36	0.991	126.32	178.9	C33	C32	C35
17	C27	1.404	117.83	179	C29	C25	C32
18	C24	1.401	122.37	178	C22	C1	C23
19	H28	1.071	115.95	−175.5	C24	C22	C27
20	H31	1.027	122.27	−178.2	C27	C29	C24
21	H30	1.079	113.84	171	C25	C23	C29
22	H26	0.959	119.33	−179.9	C23	C22	C25
23	C5	1.409	120.53	180	C1	C22	C23
24	C6	1.403	121.3	−179.5	C5	C1	C22
25	C7	1.397	121.37	0.7	C6	C5	C1
26	C10	1.486	121.97	179.4	C7	C6	C5
27	C4	1.401	121.24	179.7	C10	C7	C6
28	C3	1.407	121.6	−179.6	C4	C10	C7
29	C2	1.4	120	−2.4	C3	C4	C10
30	C12	1.397	118.91	3	C2	C3	C4
31	C11	1.409	120.86	179.5	C10	C7	C4
32	H20	1.101	126.06	−170.8	C11	C10	C12
33	H21	1.089	116.64	−179.4	C12	C2	C11
34	H13	1.099	121.52	172.4	C2	C3	C12
35	H14	1.068	123.66	175.3	C3	C4	C2
36	H15	0.991	126.32	−178.9	C4	C10	C3
37	C8	1.404	117.83	−179	C7	C6	C10
38	C9	1.401	122.37	−178	C1	C22	C5
39	H19	1.071	115.95	175.5	C9	C1	C8
40	H18	1.027	122.27	178.2	C8	C7	C9
41	H17	1.079	113.84	−171	C6	C5	C7
42	H16	0.959	119.33	179.9	C5	C1	C6
(b) Geometry definition for model with R group being 							
1	Cl45						
2	C24	1.78			Cl45		
3	O37	1.201	119.94		C24	Cl45	
4	C23	1.481	112.2	176.4	C24	Cl45	O37
5	C2	1.398	121.83	104.1	C23	C24	Cl45
6	C4	1.472	122.04	−0.4	C2	C23	C24
7	C5	1.396	119.9	−89.7	C4	C2	C23
8	C6	1.39	119.77	−179	C5	C4	C2
9	C7	1.391	120.16	0.1	C6	C5	C4
10	C8	1.391	120.03	0.0	C7	C6	C5
11	C9	1.396	119.99	−178.7	C4	C2	C5
12	H16	1.095	119.98	179.6	C9	C4	C8
13	H15	1.095	120.03	−179.8	C8	C7	C9
14	H14	1.095	119.98	−179.9	C7	C6	C8
15	H13	1.095	119.81	−179.9	C6	C5	C7
16	H12	1.095	119.99	−179.9	C5	C4	C6
17	C1	1.398	119.18	−179.7	C2	C23	C4
18	C3	1.388	120.54	0.0	C1	C2	C23
19	C19	1.398	120.26	0.0	C3	C1	C2
20	C21	1.469	120.31	−179.9	C19	C3	C1
21	C24	1.397	120.17	−47.6	C21	C19	C3
22	C27	1.39	120.04	−179.9	C24	C21	C19
23	C29	1.391	120.18	−0.2	C27	C24	C21
24	C25	1.391	119.93	0.1	C29	C27	C24
25	C23	1.397	120.2	180	C21	C19	C24
26	H26	1.096	119.87	179.8	C23	C21	C25
27	H30	1.095	120	180	C25	C29	C23
28	H32	1.095	120.04	180	C29	C27	C25
29	H31	1.095	119.82	180	C27	C24	C29
30	H28	1.096	119.86	179.8	C24	C21	C27
31	C18	1.395	117.81	180	C23	C24	C2
32	H22	1.097	120.01	−179.8	C18	C23	C19
33	H11	1.097	120.02	−180	C3	C1	C19
34	H10	1.096	119.44	−179.9	C1	C2	C3

charges were analysed in terms of their energy and geometric values.

The structures modelled in this study are shown in Figs. 1 and 2.

2.2. Molecular orbital modelling of substituted poly(p-phenylene)s

The same models were input to MOPAC version 6.0 [18], included in the Cerius 2 environment, the polymer modelling package from Molecular Simulations Inc. The method used was PM3, using the keywords 'eigenvector following' (EF) [26], high precision and a convergence criterion of 0.01 kJ mol^{-1}. For the models containing nitrogen atoms, the MMOK keyword was used for –(C=O)NH– groups. The band gaps were approximated using Koopman's [27] theorem and scaled with experimental results obtained from Vaschetto et al. [22–25].[2]

3. Results and discussion

3.1. Band gap

The geometries of the models are given in Table 1 (geometries for only two examples are included in this paper. Geometries for all models simulated are obtainable from the authors on request), where they are compared with experimental data. The atomic numbering scheme used in this study is shown in Fig. 2.

It is common in physical organic chemistry to compare

[2] Vaschetto et al. obtained a band gap energy of 2.8 eV. From the semi-empirical molecular orbital calculation using MOPAC the experimental poly(*p*-phenylene) 8.52 eV obtained a scaling factor of 0.33 and is used to scale all the other band gaps energy calculated.

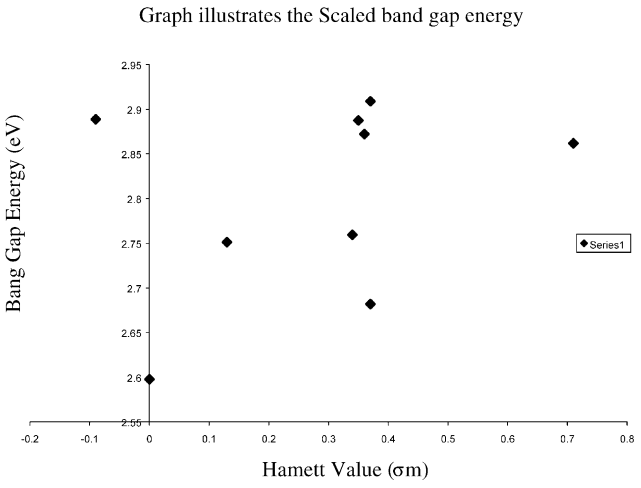

Fig. 3. The calculated band gap vs. Hammett substituent constant for the data in Table 1.

linear free energy relationships based on the Hammett equation. This approach has been extended in computational chemistry to quantitative structure activity relationships (QSAR). We have plotted the calculated (then scaled) band gaps against the Hammett substituent constant [28] for our molecules in order to see whether there is any trend with the substituent (Fig. 3), defining the hydrogen atom in the *ortho* position. For the simulation with the –(C=O)Br substituent, two calculations were performed with a different value of the RMS force. The more accurate value (0.00001 kJ mol^{-1} RMS force) gives a band gap of 8.36 eV (Table 2), compared to 8.15 eV with a 0.004 kJ mol^{-1} RMS force. Hence, we have compared our data at one value of RMS force chosen as 0.004 kJ mol^{-1} for the comparison.

Naturally, this comparison should be based on free energies but as a first approximation, semi-empirical energies can be used and the result of this is shown in Fig. 3. One may conclude from this graph that the scaled band gap values are increased from the value for the unsubstituted case, i.e. H, when the substituents are $-(C{=}O)NH_2$, –CHO, $-(C{=}O)OCH_3$, –COOH, or $-(C{=}O)NO_2$ (Table 2). Therefore, adding these substituents causes the band gap to increase and thereby reduces electrical conductivity. This is an interesting finding as these substituents were chosen to exemplify both electron donating and withdrawing properties and $-(C{=}O)NO_2$ is the most electron withdrawing group and also the most sterically hindered group. Therefore, there seems to be an effect of steric crowding on conjugation. However, there is a larger effect when the substituents are –(C=O)Cl, –(C=O)I, –(C=O)Br and $COCH_3$. The carbonyl group has the smallest effect and the –(C=O)Cl group has a much lower effect than the other halogenated compounds. It may be that with the degree of accuracy that is being used the deviation from linearity for these two is not significant. However, if this is borne out in experiment then both $-(C{=}O)CH_3$ and –(C=O)Cl would act to increase the band gap and hence reduce the conductivity of the polymer. The remaining two substituents, –(C=O)I and –(C=O)Br, have a lower band gap energy of 8.39 and 8.15 eV, respectively (Table 2) thereby increasing the conductivity when compared with the band gap energy of the experimentally calculated poly(*p*-phenylene) (8.52 eV).

Table 2
Compounds studied with calculated band gap and substituent constants

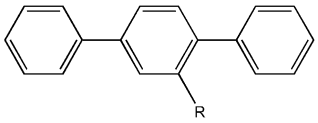

R group	Hamett value [28] σ_m	Band gap (eV)
–H	0.00	8.53
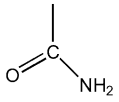	−0.09	8.72
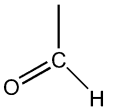	0.13	8.67
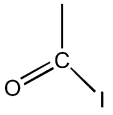	0.34	8.39
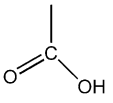	0.35	8.70
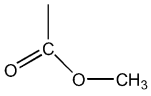	0.36	8.73
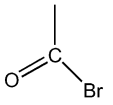	0.37	8.15, 8.36[a]
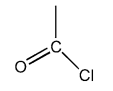	0.37	8.84
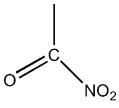	0.71	8.69

[a] RMS 0.00001 kJ mol^{-1}.

3.2. Crystal packing

Molecular mechanics analysis can provide information for structures that have been built with a periodic boundary, information that can yield the unit cell lengths (*a*, *b*, and *c*), angles (α, β and γ) volumes and densities.

Table 3
Crystal data for calculated packing for the substituted poly(*p*-phenylene)s with R groups indicated

R	*a*	*b*	*c*	*α*	*β*	*γ*	Density (g cm^{-3})	Volume (Å^3)
–H[a]	8.11	5.61	13.61	90.00	92.02	90.00	1.24	618.99
–H	4.00	5.00	12.95	84.27	92.34	89.81	1.47	257.48
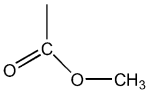	19.62	20.61	12.95	90.66	89.90	91.43	0.09	5235.01
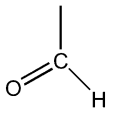	15.00	15.00	12.73	90.00	90.00	90.90	0.17	2864.40
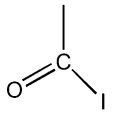	25.11	24.94	12.91	90.048	90.03	89.13	0.079	8088.07
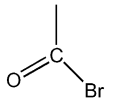	10.36	8.84	12.90	105.22	72.47	91.44	0.51	1086.29
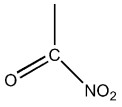	7.42	8.55	12.95	85.48	97.30	114.91	0.61	735.84
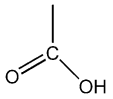	10.27	8.41	12.91	90.80	97.81	89.11	0.41	1103.97
	9.29	9.27	12.95	72.45	97.86	135.96	0.66	733.14
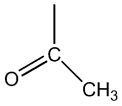	8.00	10.00	12.96	102.90	88.73	110.48	0.48	945.10
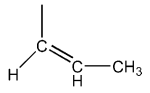	6.72	12.98	12.90	78.07	99.99	97.77	0.41	1077.3
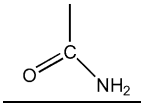	5.00	7.00	12.75	90.00	90.00	90.00	1.21	446.15

[a] Structure obtained via CSD database [21].

The calculated solid-state molecules of poly(*p*-phenylene) show a density value of 1.47 g cm^{-3}, whilst the experimental value for the density of poly(*p*-phenylene) is 1.24 g cm^{-3}. The calculated poly(*p*-phenylene) (marked as –H, see Table 3) has twisted out of plane and is occupying more space within the unit cell, while the experimental poly(*p*-phenylene) (marked as –H[a] in Table 3) is planar within its unit cell and is not occupying as much space. The significance of this observation relates to the conductivity and packing of the poly(*p*-phenylene) in the gas phase. The results obtained in the free state and in the crystal state shows the effect on the torsion angles of each type of substituted poly(*p*-phenylene) molecule. The geometries of the models are given in Table 1, where they are compared with the literature studies reported by Rietveld et al. [21]. The atomic numbering scheme used in this study is shown in Fig. 2.

3.3. Torsion angles

Torsion angles calculated for both the solid-state packing simulations using molecular mechanics and the gas phase

Table 4
Calculated torsion angles for the substituents detailed in the crystal and free state

R group	Solid-state[a]				Gas phase[b]			
	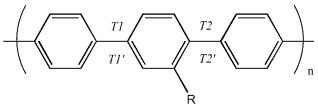				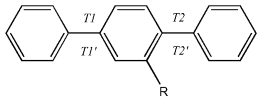			
	*T*1	*T*2	*T*1′	*T*2′	*T*1	*T*2	*T*1′	*T*2′
–H[c]	0.74	1.25	−1.25	−0.74	–	–	–	–
–H	69.24	−68.33	68.31	−69.30	0.000	0.00	0.00	0.00
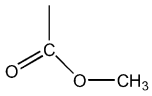	39.90	79.06	39.39	79.08	−46.77	−46.77	88.75	91.47
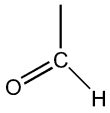	58.24	104.77	51.85	107.66	−0.078	−0.62	−86.70	−88.05
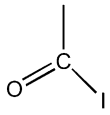	53.49	70.66	52.46	71.12	47.78	47.92	−93.17	−95.29
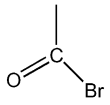	35.98	70.13	35.36	68.83	−47.79	−47.79	−59.18	−60.77
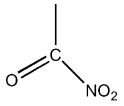	−35.75	62.24	−34.35	63.03	−47.24	−47.29	−64.37	−65.69
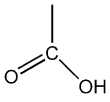	−46.21	96.44	−44.99	99.66	129.48	129.09	113.80	115.74
	−39.78	77.86	−39.09	78.46	132.37	132.35	−88.69	−89.66
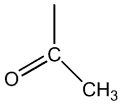	−29.82	61.94	−28.93	60.46	132.47	132.67	−95.13	−96.35
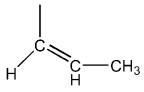	56.99	55.16	58.34	58.17	47.31	47.34	98.89	−101.06
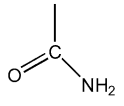	−20.34	−50.16	−21.10	−50.01	−47.54	−84.36	−47.56	−85.91

[a] RMS force was set at 0.00001 kJ mol^{-1} Å^{-1} termination criterion.
[b] Molecules were minimized by the Cerius 2 minimization (RMS force was set at 0.004 kcal mol^{-1} Å^{-1}) and then followed by geometry optimization (a convergence criterion of 0.01) method in MOPAC 6.0.
[c] Structure obtained via CSD database [21].

Table 5
Gas phase data for substituted poly(*p*-phenylene)

R group	LUMO energy (eV)	HOMO energy (eV)	MOPAC band gap energy (eV)[a]	Scaled band gap energy (eV)[b]	GRAD/GNORM (kJ mol^{-1})	Heat of formation (kJ mol^{-1})	Dipole moment (Debye)
–H	8.59	0.69	−7.90	2.60	0.007	71.60	0.00
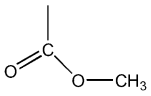	−9.26	−0.36	−8.89	2.93	0.004	32.93	2.61
	−9.42	−0.57	−8.84	2.91	0.006	34.15	2.83
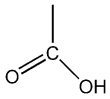	−9.42	−0.65	−8.78	2.89	0.008	−13.64	4.53
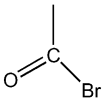	−9.14	−0.99	−8.15	2.68	0.007	43.20	3.41
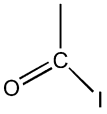	−9.46	−1.07	−8.39	2.76	0.007	60.46	3.55
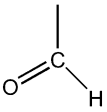	−9.05	−0.69	−8.36	2.75	0.009	40.02	2.68
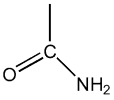	−9.20	−0.48	−9.44	3.11	0.007	36.74	3.44
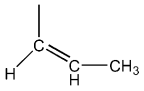	−8.99	−0.21	−8.78	2.89	0.007	81.52	0.40
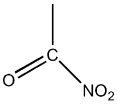	−9.57	−0.88	−8.69	2.86	0.008	39.87	4.53
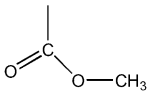	−9.29	−0.56	−8.73	2.87	0.009	−2.97	−2.03

[a] Band energy approximated as the $E_{HOMO}-E_{LUMO}$.
[b] Scaled band gap energy using literature value of 2.8 eV for poly(*p*-phenylene) [22].

using MOPAC are presented in Table 4. We have implied from the molecules built that the torsion angles should be defined as; $T1$ (atoms numbered 5, 4, 2 and 1), $T2$ (atoms numbered 3, 18, 21 and 24), $T1'$ (atoms numbered 9, 4, 2 and 17) and $T2'$ (atoms numbered 19, 18, 21 and 23). The results show that the DREIDING 2.21 force field is poor at reproducing the experimental torsion angles of poly(*p*-phenylene) (marked –H[c] see Table 4). The torsion angles for this are $T1 = 0.7°$, $T2 = 1.3°$ for the experimental and $T1 = 69.2°$, $T2 = -68.3°$ for the molecular mechanics simulation. The molecular mechanics calculations will be unlikely to give good geometries of the molecules under study, because they depend on delocalized π interactions that are not modelled by molecular mechanics. Hence, changing the parameter set will not improve the molecular mechanics models. However, the gas phase results are more in line with the experiment ($T1 = 0.0°$, $T2 = 0.0°$). Therefore, there is a need to account for the conjugation of the orbitals to produce the correct torsion angles. This means that the calculated torsion angles for the substituted

molecules in the solid-state must be judged as unreliable and it would be safer to use the gas phase values. The gas phase values for the substituted poly(*p*-phenylene)s indicate the expected trend that increasing bulk substituent causes a greater deviation from planarity. The least deviation from planarity is caused by the –CHO substituent and the other substituents deviate from planarity to approximately the same extent. This trend is reproduced in the molecular mechanics calculations with the majority of the substituents showing similar torsion angles.

3.4. Heats of formation and dipole moments

Semi-empirical analysis can allow for further information than for simple molecular mechanical studies. A useful quantity is the heat of formation, which can be deduced by using the semi-empirical package MOPAC on small and simple molecules. The results of the free state heats of formation and dipole moments are presented in Table 5. The results show that the –COOH substituted molecule has the lowest heat of formation (13.64 kJ mol^{-1}) compared with the experimental poly(*p*-phenylene) (71.60 kJ mol^{-1}). Other substituted molecules, –(C=O)CH_3, 32.93; –(C=O)Cl, 34.15; –(C=O)Br, 43.20; –(C=O)I, 60.46; –CHO, 40.02 kJ mol^{-1}) fall in between the values given above. The molecule bearing, –CH–CH=CH_2 has a heat of formation of 81.52 kcal mol^{-1} which could be accounted for by the extra bonds present in the molecule making the Gibbs free energy (ΔG^0) less favourable and hence make the heat of formation larger than the unsubstituted poly(*p*-phenylene). Assuming that the temperature and entropy are constant over the molecules in the free state then ΔG^0 can be assumed to be proportional to ΔH_f^0. On examination of Table 5 it can be seen that only the acetyl and the carboxylate substituted molecules have a negative ΔH_f^0 and therefore can be assumed to be prepared more readily than the others in the series. However, it is important not to make much of the results at this level of approximation and only consider trends.

The electric dipoles reflect the distribution of charges within the molecule. The result of the calculated dipole moments (Table 5) for the molecule which has –COOH as its substituent has the largest dipole moment at 4.53 Debye, which is higher than any of the other molecules studied and also larger than the unsubstituted poly(*p*-phenylene) which has a dipole moment of 0.00 Debye. Larger, heavier atoms such as –(C=O)I (3.52 Debye) and –(C=O)Br (3.41 Debye) also show large dipole moments.

4. Conclusions

In this study, molecular mechanics and molecular orbital methods were used to calculate physical and electronic properties for substituted poly(*p*-phenylene)s and make comparisons with experimental data of simple straight chained poly(*p*-phenylene)s from the literature. The molecular orbital methods used appear to produce more accurate results than the molecular mechanical method when they are compared with the literature experimental data. This may be due to the use of appropriate semi-empirical parameters.

In future work, we aim to model different types of substituted poly(*p*-phenylene)s in an effort to understand the solubility and physical properties of different materials and also to improve the prediction of the physicomechanical properties through modelling. The use of computer simulations and the growth of computing power will hasten the growth of this field, and further developments in this will eventually lead to accurate predictions. There is certainly room for improvement in the molecular orbital techniques used. We are currently studying the 'crystal orbital' approach to calculate solid-state properties of infinite chains and the results of this approach will be presented in future papers.

References

[1] Ivory DM, Miller GG, Sowa JM, Shacklette LW, Chance RR, Baughman RH. J Chem Phys 1979;71:1506.
[2] Ivory DM, Miller GG, Sowa JM, Shacklette LW, Chance RR, Elsenbaumer RL, Baughman RH. J Chem Soc Chem Commun 1980:348.
[3] Rabolt JF, Clarke TC, Kanazawa K, Reynolds JR, Street GB. J Chem Soc Chem Commun 1980:347.
[4] Lin JWP, Dudek LP. J Polym Sci, Polym Lett Ed 1980;18:2869.
[5] Ohsaka T, Ohnuki Y, Oyama N, Katagiri G, Kamisako K. J Electroanal Chem 1984;161:399.
[6] Edwards JH, Feast WJ, Bott DC. Polymer 1984;25:395.
[7] Feast WJ, Winter JN. J Chem Soc Chem Commun 1985;85:202.
[8] White D, Bott DC. Polym Commun 1984;25:98.
[9] Jenekhe SA. In: Benham JL, Kinstle JF, editors. Chemical reactions on polymers, ACS Symposium Series 364. Washington, DC: American Chemical Society, 1988. Chapter 32.
[10] Bredas JL. Adv Mater 1995;7:263.
[11] Salanek WR, Bredas JL. Synth Met 1994;67:15.
[12] Bredas JL. Synth Met 1997;84:3.
[13] Quattrocchi C, DosSantos DA, Bredas JL. Synth Met 1995;74:187.
[14] DosSantos DA, Bredas JL. Synth Met 1994;67:15.
[15] Beljonne D, Shuai Z, Friend RH, Bredas JL. J Chem Phys 1995; 102:2042.
[16] Cornil J, Beljonne D, Bredas JL. J Chem Phys 1995;103:834.
[17] Bredas JL, Fahlam M. Synth Met 1996;78:39.
[18] Molecular Simulations. 16 New England Executive Park, Burlington, MA 0183-5297, USA.
[19] Rappe AK, Goddard WA. J Phys Chem 1991;95:3358.
[20] Mayo SL, Olafson BD, Goddard III WA. J Phys Chem 1990;94: 8897–909.
[21] Rietveld HM, Maslen EN, Clews CJB. Acta Crystallogr, Sect B 1970;26:693.
[22] Vaschetto ME, Andrew PM, Springborg MJ. J Mol Struct (Theochem) 1999;468:181.
[23] Gin DL, Conticello CV. Trends Polym Sci 1996;4:217.
[24] Grem G, Leditzky G, Ullrich B, Leising G. Adv Mater 1992;4:36.
[25] Grem G, Leditzky G, Ullrich B, Leising G. Synth Met 1992;51:383.
[26] Baker J. J Comput Chem 1985;7:385.
[27] Koopman TA. Physica 1933;1:104.
[28] March J. Reaction mechanisms and structure, 4th ed. Advanced organic reaction. New York: Wiley, 1992. Chapter 2, p. 278–87.